Dynamic Diffusion Analysis of Chitosan-based Hydrogels Using Magnetic Resonance

R. Wong[1], C-C. Chu[2,3], C. Zhong[3], and Y. Wang[1,4]

[1]Department of Biomedical Engineering, Cornell University, Ithaca, NY, United States, [2]Department of Biomedical Engineering, Cornell Unversity, Ithaca, NY, United States, [3]Fiber Science Program, Dept. of Fiber Science and Apparel Design, Cornell University, Ithaca, NY, United States, [4]Department of Radiology, Weill Medical College of Cornell University, New York, NY, United States

Introduction: Due to their hydrophilicity, physical pliability, and biocompatibility, there is significant interest in developing biodegradable hydrogels as biological analogs to naturally formed tissue for use in regulated drug delivery, tissue engineering, and other bioengineering applications[1]. Of particular importance is the assessment and quantification of a hydrogel's interaction with water, including its absorption characteristics, physical deformation, and ultimate biodegradation under dynamic conditions[1]. In the past, the hydrogel and water interaction has been studied through traditional means including molecular probes, weight/mass variation, and morphological change[2], which do not directly probe water diffusion into and within this family of biomaterials and its relationship to their absorption characteristics. The availability of MRI technology can provide an innovative and non-destructive means to examine water perfusion and diffusion properties within this class of hydrogels for characterizing their physical and chemical structure[3,4], providing the knowledge basis for the future design of advanced generations of biomaterials.

Methods: A family of four chitosan-based biodegradable hydrogels was synthesized via photopolymerization, labeled Chitosan Gels 1-4. Chitosan Gel 1 was pre-saturated in deionized water before the trial; Chitosan Gels 2-4 were initially dry. Samples were submerged in individual sealed containers containing excess 1X PBS buffered to pH 7.4 and were immediately scanned. Subsequent scans occurred every 15 minutes thereafter up to 3 hours and every 30 minutes thereafter up to 8 hours. Air temperature was regulated by central air to 20°C and all samples and solutions were equilibrated to room temperature before the start of the trial. All imaging was performed on a clinical Signa 1.5T scanner (GE Healthcare, Milwaukee, WI). Volumetric measurements were made using 3D FIESTA (TE/TR 2.3 ms/7.6ms, Flip Angle = 60°, 128x128 matrix, FOV = 7x3.5cm, 30x1mm coronal slices). Diffusion weighted images (DWI) were acquired using Single Shot EPI (TE/TR = 2.3ms/10 sec, 128x128 matrix, FOV = 7x3.5cm, 5x1mm axial slices, b = 1000s/mm2). Proton density (PD) weighted images were acquired using Spin Echo (TE/TR = 12ms/12 se, FOV = 7x3.5cm, 5x1mm axial slices). ADC and PD measurements were acquired on an external Advantage Workstation (Version 4.3, GE Healthcare Medical, Milwaukee, WI), averaged across a ROI formed on the largest slice profile of each hydrogel.

Results: Variations in hydrogel volume (Figure 1), average apparent diffusion coefficient (Figure 2), average proton density relative to PBS (Figure 3), and calculated proton mass (Figure 4) were plotted over time. Volumetric differences in initial hydrogel volume were accounted for by scaling with initial volumes. Example cross-sectional profiles are illustrated for apparent diffusion coefficient and proton density in Figure 5. Initially dry samples (Gels 2-4) were fitted to the exponential saturation equation $x = x_s - c \exp(-t/T)$, where x represents the metric, x_s the saturation value of the metric, c a constant, T the time constant to reach saturation, and t time. Results are summarized in Table 1, indicating mostly excellent fitting to the exponential saturation, with the time constant ranging from 58min to 140min for volume change, 10min to 300min for ADC change, 27min to 69min for PD change, and 40min to 130min for proton mass change. Proton density across a horizontal profile was plotted for Gel 4 (Figure 6) and proton density at points at the center (1/2), left 1/3rd, and left 1/5th of the gel were fitted to the exponential saturation equation in Figure 7; results are summarized in Table 2 with the time constant ranging from 69min to 133min.

Discussion: The exponential saturation equation indicates that the rate of water diffusion into hydrogels is approximately determined by the remaining capacity (x_s-x) and the time constant T: $dx/dt = (x_s\text{-}x)/T$. Both the saturation metric x_s and the saturation time constant T are determined by and provide MRI characterization of hydrogels. Time constants for volume change and proton density show moderate agreement within each sample, indicating the rate of increase in volume is correlated with the rate of increase in proton density. This suggests that the intake of water is driven in part by a change in volume and ceases when volume is no longer increasing. Time constants for apparent diffusion coefficient shows little agreement with other metrics, suggesting independence between the calculated diffusion coefficient with respect to both the quantity of water intake and volume. Results indicate that a gel's chemical makeup influences time constant T and equilibrium point C for all metrics, and can be varied in the pursuit of specific absorption characteristics for specific research applications.

ADC/PD image maps and proton density profiles over time suggest water initially diffuses from the surface of the gel and propagates inward, a conclusion supported by fitted exponential models of PD at varying points within the gel. However, time constants vary little with regard to position (69min < T < 76min), suggesting that the rate at which water intake equilibrium is achieved at a specific point is independent of location. This suggests that the absorption rate of any portion of a hydrogel are equal, and several locations can be represented by similar time-shifted exponential fitting functions.

This study identifies three metrics of hydrogel absorption, volume, apparent diffusion coefficient, and proton density, and demonstrates the behavioral variability that can be achieved by altering a hydrogel's composition. Further, this study explores the rate of water uptake at specific points within the hydrogel, and provides insight into the uniformity of absorption characteristics within a homogenous body. Both have a direct impact on the performance-directed synthesis of hydrogels and demonstrate the use of MRI as a tool in evaluating hydrogel absorption.

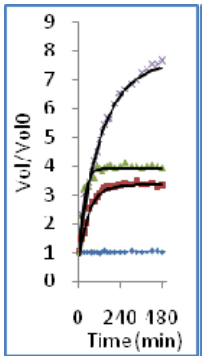

Figure 1. Rel volume change over time.

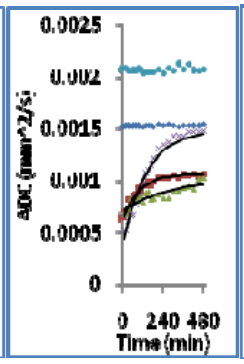

Figure 2. Average ADC change over time.

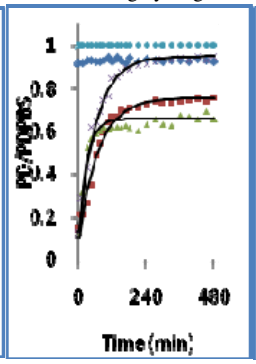

Figure 3. Average PD relative to PBS over time.

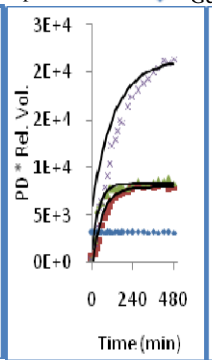

Figure 4. Calculated proton mass over time.

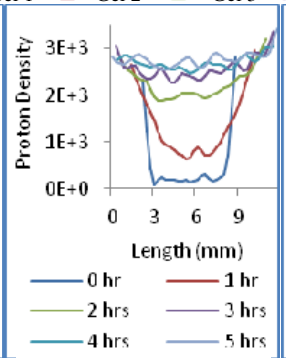

Figure 6. PD across center profile of Gel 4.

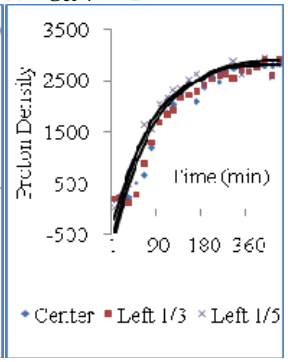

Figure 7. Gel 4 proton density, at varying locations,

	Rel.Volume			Avg.ADC			Avg. Rel. PD			Rel.Proton Mass		
Gel	**C** (mm^2)	**T**(min)	R^2	**C** (mm^2/s)	**T** (min)	R^2	**C**	**T** (min)	R^2	**C (n)**	**T** (min)	R^2
2	2.49	57.98	0.99	0.00040	101.50	0.97	0.665	**69.25**	0.98	8552	57.64	0.93
3	2.96	28.09	0.97	0.00031	**298.47**	0.75	0.545	27.49	0.94	7146	39.64	0.95
4	**6.24**	**142.68**	0.99	**0.00104**	145.03	0.95	**0.826**	62.51	0.99	**15400**	**132.37**	0.74

Table 1. Fit parameters for dry gel samples. Largest values are highlighted.

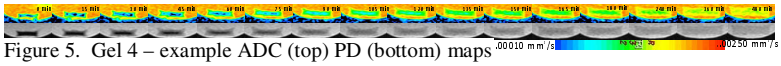

Figure 5. Gel 4 – example ADC (top) PD (bottom) maps

	Proton Density Gel 4		
Loc.	**C (n)**	**T** (min)	R^2
1/2	3328	68.83	0.88
1/3	3541	76.07	0.90
1/5	1125	73.62	0.97

Table 2. Fit parameters for Gel 4 at varying locations within the sample.

References: [1] Hoffman, A.S., et al. *Ann NY Acad Sci* 944: 52-73, 2001. [2] Qu, X., et al, *J Appl Polym Sci* 74:3186-2192, 1999. [3] Baille, W.E., et al, *Biomacromolecules* 3: 214-218:, 2002. [4] Gordon, M.J., et al, *Biotechnol Bioeng* 64: 259-467, 2000.